Dynamic Characteristics of an Eccentric Crack in a Functionally Graded Piezoelectric Ceramic Strip

Jeong Woo Shin*
Korea Aerospace Research Institute,
45 Eoeun-Dong, YouSeong-Gu, Daejeon, 305-333, Korea.
Tae-Uk Kim
Korea Aerospace Research Institute,
45 Eoeun-Dong, YouSeong-Gu, Daejeon, 305-333, Korea.
Sung Chan Kim
Korea Aerospace Research Institute,
45 Eoeun-Dong, YouSeong-Gu, Daejeon, 305-333, Korea

The dynamic response of an eccentric Griffith crack in functionally graded piezoelectric ceramic strip under anti-plane shear impact loading is analysed using integral transform method. Laplace transform and Fourier transform are used to reduce the problem to two pairs of dual integral equations, which are then expressed to Fredholm integral equations of the second kind. We assume that the properties of the functionally graded piezoelectric material vary continuously along the thickness. The impermeable crack boundary condition is adopted. Numerical values on the dynamic stress intensity factors are presented for the functionally graded piezoelectric material to show the dependence of the gradient of material properties and electric loadings.

Key Words : Piezoelectric, Eccentric Crack, FGM (Functionally Graded Material), DSIF (Dynamic Stress Intensity Factor)

Nomenclature

c_{44} : Elastic modulus
d_{11} : Dielectric permittivity
D_{ji} : Electric displacements
e_{15} : Piezoelectric constant
E_{ki} : Electric fields
e : Eccentricity off the center line
u_{ki} : Displacements vector
β : Non-homogeneous material constant
ρ : Material density
σ_{zji} : Stress components
ϕ_i : Electric potential

* Corresponding Author,
E-mail : jeongdal@kari.re.kr
TEL : +82-42-860-2026; **FAX** : +82-42-860-2009
Korea Aerospace Research Institute, 45 Eoeun-Dong, YouSeong-Gu, Daejeon, 305-333, Korea. (Manuscript **Received** February 13, 2004; **Revised** May 31, 2004)

1. Introduction

With the increase of smart structures, piezoelectric materials as actuating and sensing device have been widely used. In the use of piezoelectric structures, the dynamic loading is dominant and much attention have been paid to their dynamic fracture behavior. Shindo and Ozawa (1990) first investigated the steady response of a cracked piezoelectric material under the action of incident plane harmonic waves. Chen and Yu (1997) obtained the solution of a finite crack in an infinite piezoelectric material under anti-plane dynamic electro-mechanical impact using integral transform method. Axisymmetric vibration of piezo-composite hollow cylinder was studied by Paul and Nelson (1996). The dynamic representation formulas and fundamental solutions for

piezoelectricity was proposed by Khutoryansky and Sosa (1995). The dynamic response of a cracked dielectric medium under the action of harmonic waves in a uniform electric field was studied by Shindo et al.(1996). Narita and Shindo (1998) investigated the scattering of Love waves by a surface-breaking crack normal to the interface in a piezoelectric layer over an elastic half plane. Li and Mataga (1996a, 1996b) studied the semi-infinite propagating crack in a piezoelectric material with electrode boundary and vacuum boundary conditions on the crack surface. Chen (1998) obtained the solution of the infinite piezoelectric strip parallel to the crack under anti-plane shear impact electro-mechanical loading using integral transform method. Shin et al.(2001) obtained the solution of piezoelectric strip with an eccentric crack under anti-plane shear impact loading using integral transform method. Recently, fracture mechanics researches of functionally graded piezoelectric material are presented. Li and Weng (2002) studied anti-plane crack problem in functionally graded piezoelectric strip. Shin and Kim (2003) obtained the solution of the functionally graded piezoelectric strip with an eccentric crack under anti-plane shear. Transient response of functionally graded piezoelectric body with crack was analysed by Shin et al.(2003).

In this paper, we study the problem of a finite eccentric crack off the center line in a functionally graded piezoelectric ceramic strip under anti-plane shear impact loading by the dynamic theory of linear electroelasticity. We assume that the properties of the functionally graded piezoelectric ceramic strip vary continuously along the thickness. We adopt the impermeable crack boundary condition which is more suitable in this paper rather than permeable crack boundary condition (Xu and Rajapakse, 2001). Laplace transform and Fourier transform are used to reduce the problem to two pairs of dual integral equations, which are then expressed to Fredholm integral equations of the second kind. Numerical results for the dynamic stress intensity factor are shown graphically.

2. Problem Statement and Formulation

Consider a functionally graded piezoelectric body in the form of an infinitely long strip containing a finite eccentric crack off the center line subjected to mechanical and electric Heaviside step pulse loadings, as shown in Fig. 1. A set of cartesian coordinates (x, y, z) is attached to the center of the crack. The piezoelectric ceramic strip poled with z-axis occupies the region $(-\infty<x<\infty, -h_2\leq y\leq h_1, 2h=h_1+h_2)$, and is thick enough in the z-direction to allow a state of anti-plane shear impact. For convenience, we assume that upper ($y\geq 0$, thickness h_1) and lower ($y\leq 0$, thickness h_2) regions of the strip cracked with the eccentricity e off the center line have different thicknesses but are consisted of the same functionally graded materials. The crack is situated along the virtual interface line $(-a\leq x\leq a, y=0)$. Because of the symmetry in geometry and loading, it is sufficient to consider only the right-hand half body.

We assume that the properties of the functionally graded piezoelectric ceramic strip vary continuously along the thickness and are simplified as follows (Erdogan, 1985),

$$c_{44}=c_{44}^0 e^{\beta y} \tag{1}$$

$$d_{11}=d_{11}^0 e^{\beta y} \tag{2}$$

$$e_{15}=e_{15}^0 e^{\beta y} \tag{3}$$

where c_{44}, d_{11} and e_{15} are the elastic modulus, the dielectric permittivity and the piezoelectric

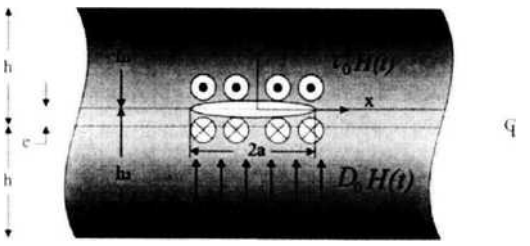

Fig. 1 A functionally graded piezoelectric ceramic strip with an eccentric crack: defintion of geometry and loading

constant, respectively. c_{44}^0, d_{11}^0 and e_{15}^0 are material properties at $y=0$, and β is the non-homogeneous material constant.

The piezoelectric boundary value problem is simplified considerably if we consider only the out-of-plane displacement and the in-plane electric fields such that

$$u_{xi}=u_{yi}=0,\ u_{zi}=w_i(x,\ y,\ t) \tag{4}$$

$$\begin{aligned} E_{xi}&=E_{xi}(x,\ y,\ t)\\ E_{yi}&=E_{yi}(x,\ y,\ t),\ E_{zi}=0 \end{aligned} \tag{5}$$

where u_{ki} and $E_{ki}(k=x,\ y,\ z)$ are displacements and electric fields, respectively. Subscript $i(i=1,\ 2)$ stands for upper and lower regions, respectively.

In this case, the constitutive relations become

$$\sigma_{zji}(x,\ y,\ t)=c_{44}w_{i,j}+e_{15}\phi_{i,j} \tag{6}$$

$$D_{ji}(x,\ y,\ t)=e_{15}w_{i,j}-d_{11}\phi_{i,j} \tag{7}$$

where σ_{zji}, $D_{ji}(j=x,\ y)$ and ϕ_i are the stress components, the electric displacements and the electric potential, respectively.

The dynamic anti-plane governing equations for functionally graded piezoelectric materials are simplified to

$$\begin{aligned} &c_{44}\nabla^2 w_i+e_{15}\nabla^2\phi_i+\beta\left(c_{44}\frac{\partial w_i}{\partial y}+e_{15}\frac{\partial\phi_i}{\partial y}\right)\\ &=\rho\frac{\partial^2 w_i}{\partial t^2} \end{aligned} \tag{8}$$

$$e_{15}\nabla^2 w_i-d_{11}\nabla^2\phi_i+\beta\left(e_{15}\frac{\partial w_i}{\partial y}-d_{11}\frac{\partial\phi_i}{\partial y}\right)=0 \tag{9}$$

where $\nabla^2=\partial^2/\partial x^2+\partial^2/\partial y^2$ and ρ is a material density. We also assume the material density is as follows,

$$\rho=\rho^0 e^{\beta y} \tag{10}$$

From Eqs. (8) and (9), we can obtain the equation of wave motion in a form,

$$\nabla^2 w_1+\beta\frac{\partial w_i}{\partial y}=\frac{1}{c_2^2}\frac{\partial^2 w_i}{\partial t^2} \tag{11}$$

where $c_2=\sqrt{\mu_0/\rho^0}$ and $\mu_0=c_{44}^0+e_{15}^{02}/d_{21}^0$.

The Laplace transform of Eq. (11) is in the form,

$$\nabla^2 w_i^*+\beta\frac{\partial w_i^*}{\partial y}=\frac{p^2}{c_2^2}w_i^* \tag{12}$$

where

$$w_i^*(x,\ y,\ p)=\int_0^\infty w_i(x,\ y,\ t)\,e^{-pt}dt \tag{13}$$

$$w_i(x,\ y,\ t)=\frac{1}{2\pi i}\int_{c-i\infty}^{c+i\infty} w_i^*(x,\ y,\ p)\,e^{pt}dp \tag{14}$$

The superscript $*$ stands for the Laplace transform domain.

A Fourier transform is applied to the Laplace transform of Eqs. (9), and (12), and the results are

$$\begin{aligned} &w_i^*(x,\ y,\ p)\\ &=\frac{2}{\pi}\int_0^\infty[A_{1i}(s,\ p)\,e^{-q_1 y}+A_{2i}(s,\ p)\,e^{-q_2 y}]\cos(sx)\,ds \end{aligned} \tag{15}$$

$$\begin{aligned} &\phi_i^*(x,\ y,\ p)\\ &=\frac{2}{\pi}\frac{e_{15}^0}{d_{11}^0}\int_0^\infty[A_{1i}(s,\ p)\,e^{-q_1 y}+A_{2i}(s,\ p)\,e^{q_2 y}]\cos(sx)\,ds\\ &\quad+\frac{2}{\pi}\int_0^\infty[B_{1i}(s,\ p)\,e^{-p_1 y}+B_{2i}(s,\ p)\,e^{p_2 y}]\cos(sx)\,ds \end{aligned} \tag{16}$$

where

$$q_1=\delta+\frac{\beta}{2},\ q_2=\delta-\frac{\beta}{2} \tag{17}$$

$$p_1=\lambda+\frac{\beta}{2},\ p_2=\lambda-\frac{\beta}{2} \tag{18}$$

$$\delta=\sqrt{\gamma^2+\frac{\beta^2}{4}},\ \lambda=\sqrt{s^2+\frac{\beta^2}{4}} \tag{19}$$

$$\gamma=\sqrt{s^2+\frac{p^2}{c_2^2}} \tag{20}$$

A_{ji} and $\beta_{ji}(j=1,\ 2)$ are the unknowns to be solved.

Substituting Eqs. (15) and (16) into Eqs. (6) and (7) in the Laplace transform domain, we have the followings

$$\begin{aligned} &\sigma_{yzi}^*(x,\ y,\ p)\\ &=\mu_0\frac{2}{\pi}\int_0^\infty[-A_{1i}(s,\ p)\,q_1 e^{-q_1 y}+A_{2i}(s,\ p)\,q_2 e^{q_2 y}]\cos(sx)\,ds\\ &\quad+e_{15}^0\frac{2}{\pi}\int_0^\infty[-B_{1i}(s,\ p)\,p_1 e^{-p_1 y}+B_{2i}(s,\ p)\,p_2 e^{p_2 y}]\cos(sx)\,ds \end{aligned} \tag{21}$$

$$\begin{aligned} &D_{yi}^*(x,\ y,\ p)\\ &=-d_{11}^0\frac{2}{\pi}\int_0^\infty[B_{1i}(s,\ p)\,p_1 e^{-p_1 y}+B_{2i}(s,\ p)\,p_2 e^{p_2 y}]\cos(sx)\,ds \end{aligned} \tag{22}$$

The boundary conditions in the Laplace transform domain can be written as

$$\begin{cases} \sigma_{yzi}^*(x, 0, p) = -\tau_0/p & (0 \le x < a) \\ w_1^*(x, 0, p) = w_2^*(x, 0, p) & (a \le x < \infty) \end{cases} \quad (23)$$

$$\begin{cases} D_{yi}^*(x, 0, p) = -D_0/p & (0 \le x < a) \\ \phi_1^*(x, 0, p) = \phi_2^*(x, 0, p) & (a \le x < \infty) \end{cases} \quad (24)$$

$$\begin{cases} \sigma_{yz1}^*(x, 0, p) = \sigma_{yz2}^*(x, 0, p) \\ D_{y1}^*(x, 0, p) = D_{y2}^*(x, 0, p) & (a \le x < \infty) \end{cases} \quad (25)$$

$$\begin{cases} \sigma_{yz1}^*(x, h_1, p) = \sigma_{yz2}^*(x, -h_2, p) = 0 \\ D_{y1}^*(x, h_1, p) = D_{y2}^*(x, -h_2, p) = 0 \end{cases} \quad (26)$$

where τ_0 and D_0 are a uniform shear traction and electric displacement, respectively.

By applying the edge loading conditions Eq. (26), the unknowns in Eqs. (21) and (22) are evaluated as follows,

$$\begin{aligned} A_{21}(s, p) &= ke^{-2\delta h_1} A_{11}(s, p) \\ A_{22}(s, p) &= ke^{2\delta h_2} A_{22}(s, p) \end{aligned} \quad (27)$$

$$\begin{aligned} B_{21}(s, p) &= fe^{-2\lambda h_1} B_{11}(s, p) \\ B_{22}(s, p) &= fe^{2\lambda h_2} B_{22}(s, p) \end{aligned} \quad (28)$$

where

$$k = \frac{q_1}{q_2}, \quad f = \frac{p_1}{p_2} \quad (29)$$

The continuity conditions of Eq. (25) lead to the following relations between the unknowns,

$$\begin{aligned} &k\{A_{11}(s, p) - A_{12}(s, p)\} \\ &= A_{21}(s, p) - A_{22}(s, p) \end{aligned} \quad (30)$$

$$\begin{aligned} &f\{B_{11}(s, p) - B_{12}(s, p)\} \\ &= B_{21}(s, p) - B_{22}(s, p) \end{aligned} \quad (31)$$

It is convenient to use the following definitions,

$$\begin{aligned} A_{11}(s, p) - A_{12}(s, p) &= M_A(s, p) \\ B_{11}(s, p) - B_{12}(s, p) &= M_B(s, p) \end{aligned} \quad (32)$$

Using the Eqs. (27) ~ (32), we can obtain the following relations,

$$A_{11}(s, p) = \frac{1 - e^{-2\delta h_2}}{1 - e^{-4\delta h}} M_A(s, p) \quad (33)$$

$$A_{12}(s, p) = \frac{e^{-4\delta h} - e^{-2\delta h_2}}{1 - e^{-4\delta h}} M_A(s, p) \quad (34)$$

$$A_{21}(s, p) = k \frac{e^{-2\delta h_1} - e^{-4\delta h}}{1 - e^{-4\delta h}} M_A(s, p) \quad (35)$$

$$A_{22}(s, p) = -k \frac{1 - e^{-2\delta h_1}}{1 - e^{-4\delta h}} M_A(s, p) \quad (36)$$

$$B_{11}(s, p) = \frac{1 - e^{-2\lambda h_2}}{1 - e^{-4\lambda h}} M_B(s, p) \quad (37)$$

$$B_{12}(s, p) = \frac{e^{-4\lambda h} - e^{-2\lambda h_2}}{1 - e^{-4\lambda h}} M_B(s, p) \quad (38)$$

$$B_{21}(s, p) = f \frac{e^{-2\lambda h_1} - e^{-4\lambda h}}{1 - e^{-4\lambda h}} M_B(s, p) \quad (39)$$

$$B_{22}(s, p) = -f \frac{1 - e^{-2\lambda h_1}}{1 - e^{-4\lambda h}} M_B(s, p) \quad (40)$$

The two mixed boundary conditions of Eqs. (23) and (24) lead to two simultaneous dual integral equations in the forms,

$$\begin{aligned} &\int_0^\infty s f(s, p) M_A(s, p) \cos(sx)\, ds \\ &= \frac{\pi}{2} \frac{1}{p\mu_0} \left(\tau_0 + \frac{e_{15}^0}{d_{11}^0} D_0 \right), \quad (0 \le x < a) \\ &\int_0^\infty M_A(s, p) \cos(sx)\, ds = 0, \quad (a \le x < \infty) \end{aligned} \quad (41)$$

where

$$f(s, p) = \frac{q_1}{s} \frac{(1 - e^{-2\delta h_1})(1 - e^{-2\delta h_2})}{(1 - e^{-4\delta h})} \quad (42)$$

$$\begin{aligned} &\int_0^\infty s g(s) M_B(s, p) \cos(sx)\, ds \\ &= -\frac{\pi}{2} \frac{D_0}{p d_{11}^0}, \quad (0 \le x < a) \\ &\int_0^\infty M_B(s, p) \cos(sx)\, ds = 0, \quad (a \le x < \infty) \end{aligned} \quad (43)$$

where

$$g(s) = \frac{p_1}{s} \frac{(1 - e^{-2\lambda h_1})(1 - e^{-2\lambda h_2})}{1 - e^{-4\lambda h}} \quad (44)$$

The sets of two simultaneous dual integral Eqs. (41) and (43) may be solved by using new functions $\Phi_1^*(\xi, p)$ and $\Phi_2^*(\xi, p)$ defined by

$$\begin{aligned} M_A(s, p) &= \int_0^a \xi \Phi_1^*(\xi, p) J_0(s\xi)\, d\xi \\ M_B(s, p) &= \int_0^a \xi \Phi_2^*(\xi, p) J_0(s\xi)\, d\xi \end{aligned} \quad (45)$$

where $J_0(\ )$ is the zero-order Bessel function of the first kind.

Inserting Eq. (45) into Eqs. (41) and (43), we can find that the auxiliary functions $\Phi_1^*(\xi, p)$ and $\Phi_2^*(\xi, p)$ are given by Fredholm integral equations of the second kind in the forms,

$$\Phi_1^*(\xi, p)+\int_0^a K_1(\xi, \eta, p)\,\Phi_1^*(\eta, p)\,d\eta = \frac{\pi}{2}\frac{1}{p\mu_0}\left(\tau_0+\frac{e_{15}^0}{d_{21}^0}D_0\right) \tag{46}$$

$$\Phi_2^*(\xi)+\int_0^a K_2(\xi, \eta)\,\Phi_2^*(\eta)\,d\eta = -\frac{\pi}{2}\frac{d_0}{pd_{11}^0} \tag{47}$$

where

$$K_1(\xi, \eta, p) = \eta\int_0^\infty s\{f(s, p)-1\}J_0(s\eta)J_0(s\xi)\,ds \tag{48}$$

$$K_2(\xi, \eta) = \eta\int_0^\infty s\{g(s)-1\}J_0(s\eta)J_0(s\xi)\,ds \tag{49}$$

We introduce the following dimensionless variables and functions for numerical analysis,

$$s=\frac{S}{a},\ \beta=\frac{B}{a},\ \gamma=\frac{\Gamma}{a},\ \delta=\frac{\Delta}{a},\ \lambda=\frac{\Lambda}{a} \tag{50}$$

$$\eta=aH,\ \xi=a\Xi \tag{51}$$

$$\Phi_1^*(\xi, p)=\frac{\pi}{2}\frac{1}{p\mu_0}\left(\tau_0+\frac{e_{15}^0}{d_{11}^0}D_0\right)\frac{\Psi_1^*(\Xi, p)}{\sqrt{\Xi}} \tag{52}$$

$$\Phi_2^*(\xi)=-\frac{\pi}{2}\frac{D_0}{pd_{11}^0}\frac{\Psi_2^*(\Xi)}{\sqrt{\Xi}} \tag{53}$$

Substituting Eqs. (50) ~ (53) into Eqs. (46) ~ (49), we can obtain Fredholm integral equations of the second kind in the forms,

$$\Psi_1^*(\Xi, p)+\int_0^1 L_1(\Xi, H, p)\,\Psi_1^*(H, p)\,dH=\sqrt{\Xi} \tag{54}$$

$$\Psi_2^*(\Xi)+\int_0^1 L_2(\Xi, H)\,\Psi_2^*(H)\,dH=\sqrt{\Xi} \tag{55}$$

where

$$L_1(\Xi, H, p) = \sqrt{\Xi H}\int_0^\infty S\{f\left(\frac{S}{a}, p\right)-1\}J_0(SH)J_0(S\Xi)\,dS \tag{56}$$

$$L_2(\Xi, H) = \sqrt{\Xi H}\int_0^\infty S\{g\left(\frac{S}{a}\right)-1\}J_0(SH)J_0(S\Xi)\,dS \tag{57}$$

$$f\left(\frac{S}{a}, p\right)=\frac{Q_1}{S}\frac{(1-e^{-2\Delta\left(\frac{h}{a}+\frac{e}{a}\right)})(1-e^{-2\Delta\left(\frac{h}{a}-\frac{e}{a}\right)})}{1-e^{-4\Delta\frac{h}{a}}} \tag{58}$$

$$g\left(\frac{S}{a}\right)=\frac{P_1}{S}\frac{(1-e^{-2\Delta\left(\frac{h}{a}+\frac{e}{a}\right)})(1-e^{-2\Delta\left(\frac{h}{a}-\frac{e}{a}\right)})}{1-e^{-4\Delta\frac{h}{a}}} \tag{59}$$

$$Q_1=\Delta+\frac{B}{2},\ P_2=\Lambda-\frac{B}{2} \tag{60}$$

e denotes the eccentricity.

3. Dynamic Intensity Factors

The mode III intensity factors in the Laplace transform domain, $K_{III}^{\tau*}(p)$ and $K_{III}^{D*}(p)$, are defined and determined in the forms

$$K_{III}^{\tau*}(p)=\lim_{x\to a^+}\sqrt{2\pi(x-a)}\{\sigma_{yzi}^*(x, 0, p)-i\sigma_{xzi}^*(x, 0, p)\} = \frac{1}{p}\left[\Psi_1^*(1, p)\left(\tau_0+\frac{e_{15}^0}{d_{11}^0}D_0\right)-\frac{e_{15}^0}{d_{11}^0}D_0\Psi_2^*(1)\right]\sqrt{\pi a} \tag{61}$$

$$K_{III}^{D*}(p)=\lim_{x\to a^+}\sqrt{2\pi(x-a)}\{D_{yi}^*(x, 0, p)-iD_{xi}^*(x, 0, p)\} = \frac{1}{p}D_0\Psi_2^*(1)\sqrt{\pi a} \tag{62}$$

From the inverse Laplace transform of Eqs. (61) and (62), we can obtain the dynamic intensity factors in the physical space in the forms,

$$K_{III}^{\tau}(t)=\left[\left(\tau_0+\frac{e_{15}^0}{d_{11}^0}D_0\right)M(t)-\frac{e_{15}^0}{d_{11}^0}\Psi_2^*(1)D_0H(t)\right]\sqrt{\pi a} \tag{63}$$

$$K_{III}^{D}(t)=\Psi_2^*(1)D_0H(t)\sqrt{\pi a} \tag{64}$$

where

$$M(t)=\frac{1}{2\pi i}\int_{c-i\infty}^{c+i\infty}\frac{\Psi_1^*(1, p)}{p}e^{pt}dp \tag{65}$$

in which the functions $\Psi_1^*(1, p)$ and $\Psi_2^*(1)$ can be calculated from Eqs. (54) and (55), respectively.

4. Discussions

4.1 Correctness of results

The solution of an infinite homogeneous piezoelectric strip containing a central crack parallel to the strip edges ($e=0$ and $\beta=0$) can be derived from Eqs. (54) and (55). In the case, the kernel functions $L_1(\Xi, H, p)$ and $L_2(\Xi, H)$ can be obtained as

$$L_1(\Xi, H, p) = \sqrt{\Xi H}\int_0^\infty S\{f\left(\frac{S}{a}, p\right)-1\}J_0(SH)J_0(S\Xi)\,dS \tag{66}$$

$$L_2(\Xi, H) = \sqrt{\Xi H}\int_0^\infty S\{g\left(\frac{S}{a}\right)-1\}J_0(SH)J_0(S\Xi)\,dS \tag{67}$$

where

$$f\left(\frac{S}{a}, p\right)=\frac{\Gamma[1-\exp(-2\Gamma h/a)]}{S[1+\exp(-2\Gamma h/a)]} \tag{68}$$

$$g\left(\frac{S}{a}\right)=\frac{1-\exp(-2Sh/a)}{1+\exp(-2Sh/a)} \tag{69}$$

Equations (66) and (67) are the same as those of Chen (1998).

In case of infinite functionally graded piezoelectric medium containing a finite crack ($e=0$ and $h\rightarrow\infty$), we find the kernel functions $L_1(\Xi, H, p)$ and $L_2(\Xi, H)$ in the forms,

$$L_1(\Xi, H, p)=\sqrt{\Xi H}\int_0^\infty S\{Q_1/S-1\}J_0(SH)J_0(S\Xi)\,dS \tag{70}$$

$$L_2(\Xi, H)=\sqrt{\Xi H}\int_0^\infty S\{P_1/S-1\}J_0(SH)J_0(S\Xi)\,dS \tag{71}$$

This solution agrees with those of Shin et al. (2003).

4.2 Numerical results of dynamic stress intensity factor

The dynamic intensity factors, Eqs. (63) and (64), are computed numerically by Gaussian quadrature formulas. The inverse Laplace transformation is carried out by the numerical method developed by Miller and Guy (1966). We assume that piezoelectric material properties at $y=0$ are same as PZT-5H which are as follows,

$$c_{44}=2.3\times10^{10}(\mathrm{N/m^2}),\ e_{15}=17.0(\mathrm{C/m^2})$$
$$d_{11}=150.4\times10^{-10}(\mathrm{C/Vm}) \tag{72}$$

where N, C and V are the force in Newtons, the charge in coulombs and the electric potential in volts, respectively.

From Figs. 2~5, a general feature of the curves is observed: the normalized dynamic stress intensity factor (DSIF) rise rapidly with time, reaching a peak, then decrease in magnitude to reach static values. Figure 2 displays the variation of the DSIF $K_{III}/\tau_0\sqrt{\pi a}$ against normalized time c_2t/a with various a/h values at $B=0.5$ and $e/h=0.4$ under $\tau_0=3.2\times10^6$ N/m^2 and $D_0=4.8\times10^{-4}$ C/m^2. Peak values of the DSIF increase as crack length increases. Figure 3 shows the variation of the normalized DSIF $K_{III}/\tau_0\sqrt{\pi a}$ against normalized time c_2t/a with various e/h values at $B=1.0$ and $a/h=0.2$ under $\tau_0=3.2\times10^6$ N/m^2 and $D_0=4.8\times10^{-4}$ C/m^2. In this case, Peak values of the DSIF increase as eccentricity of crack location increases.

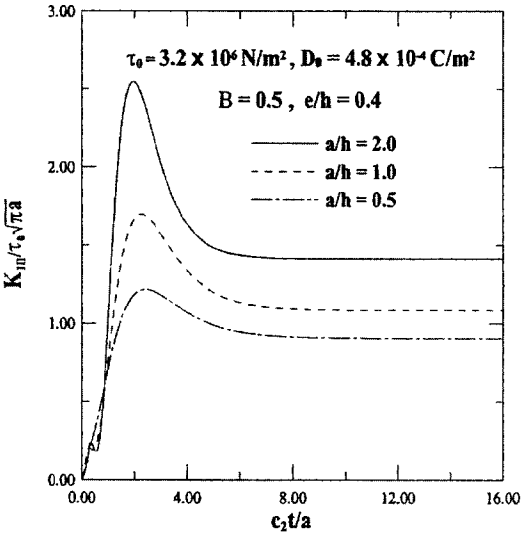

Fig. 2 Dynamic stress intensity factor for various a/h values at $B=0.5$ and $e/h=0.4$ under $\tau_0=3.2\times10^6$ N/m^2 and $D_0=4.8\times10^{-4}$ C/m^2

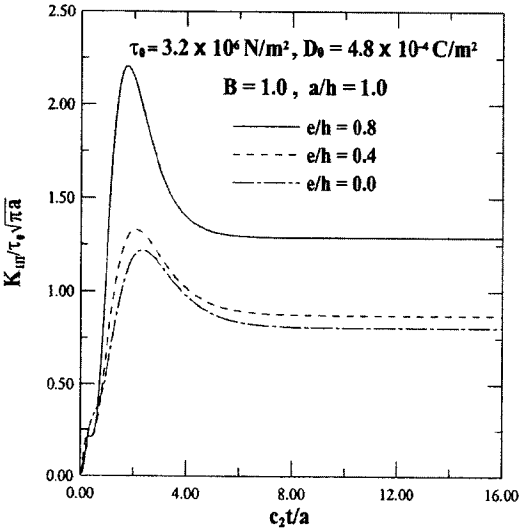

Fig. 3 Dynamic stress intensity factor for various e/h values at $B=1.0$ and $a/h=1.0$ under $\tau_0=3.2\times10^6$ N/m^2 and $D_0=4.8\times10^{-4}$ C/m^2

The effect of FGPM (functionally graded piezoelectric material) on the variation of DSIF $K_{III}/\tau_0\sqrt{\pi a}$ is shown in Fig. 4. The other parameters are chosen as $e/h=0.4$, $a/h=1.0$, $\tau_0=3.2\times10^6$ N/m^2 and $D_0=4.8\times10^{-4}$ C/m^2. Peak values of the DSIF decrease as B value increases. We can show that increasing the FGPM gradient (B) is helpful to the reduction of the DSIF. It is well-known that the SIF of functionally graded material decreases as the gradient of the material properties increases.

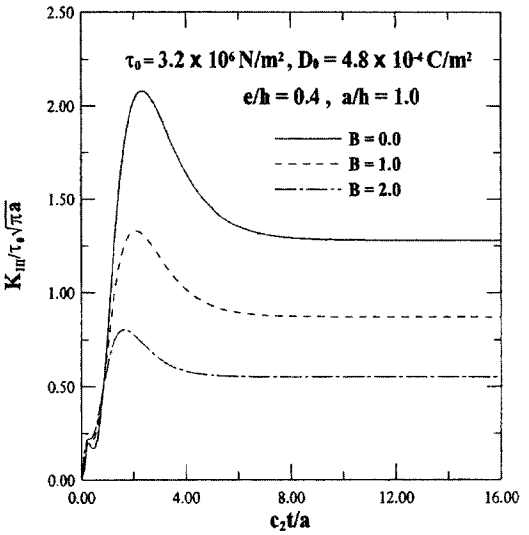

Fig. 4 Dynamic stress intensity factor for various B values at $e/h=0.4$ and $a/h=1.0$ under $\tau_0=3.2\times10^6$ N/m^2 and $D_0=4.8\times10^{-4}$ C/m^2

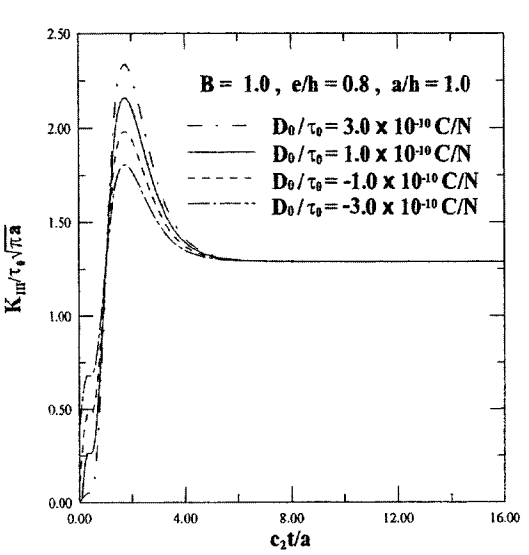

Fig. 5 Dynamic stress intensity factor for various D_0/τ_0 values at $B=1.0$, $e/h=0.8$ and $a/h=1.0$

Figures 2~4 also show that the larger values of a/h, e/h and B, the faster time arriving at peak values. Figure 5 shows the variations of the DSIF $K_{III}/\tau_0\sqrt{\pi a}$ against normalized time c_2t/a with various D_0/τ_0 values at $B=1.0$, $e/h=0.8$ and $a/h=1.0$. Peak values of the DSIF increase as the positive D_0/τ_0 value increases, but peak values decrease when the negative D_0/τ_0 value increases. It shows that the negative D_0/τ_0 values also helps the reduction of the DSIF.

5. Conclusions

The electroelastic problem of an eccentric crack off the center line in a functionally graded piezoelectric ceramic strip under anti-plane impact shear was analyzed by the integral transform approach. The properties and mass density of the functionally graded piezoelectric material vary continuously along the thickness. The impermeable crack boundary condition is adopted. The Fredholm integral equations are solved numerically. The traditional concept of linear elastic fracture mechanics is extended to include the piezoelectric effects and the results are expressed in terms of the dynamic stress intensity factor and dynamic electric displacement intensity factor. The DSIF is dependent on both stress and electric impact loads, but dynamic electric displacement intensity factor is only related to the electric impact loading. The DSIF rise rapidly with time, reaching a peak, then decrease in magnitude to reach static values. The computed results show that the DSIF can be greatly reduced by increasing the gradient of the material properties and negative electric displacement. The peak values of the DSIF increase as the eccentricity of crack location and crack length increase.

References

Chen, Z. T. and Yu, S. W., 1997, "Anti-plane

Dynamic Fracture Mechanics in Piezoelectric Materials," *International Journal of Fracture*, Vol. 85, pp. L3~L12.

Chen, Z. T., 1998, "Crack Tip Field of an Infinite Piezoelectric Strip Under Anti-plane Impact," *Mechanics Research Communications*, Vol. 25, pp. 313~319.

Erdogan, F., 1985, "The Crack Problem for Bonded Nonhomogeneous Materials Under Anti-plane Shear Loading," *ASME Journal of Applied Mechanics*, Vol. 52, pp. 823~828.

Khutoryansky, N. M. and Sosa, H., 1995, "Dynamic Representation Formulas and Fundamental Solutions for Piezoelectricity," *International Journal of Solids and Structures*, Vol. 32, pp. 3307~3325.

Li, C. and Weng, G. J., 2002, "Antiplane Crack Problem in Functionally Graded Piezoelectric Materials," *ASME, Journal of Applied Mechanics*, Vol. 69, pp. 481~488.

Li, S. and Mataga, PA., 1996, "Dynamic Crack Propagation in Piezoelectric Materials - Part I. Electrode Solution," *Journal of the Mechanics and Physics of Solids*, Vol. 44, No. 11, pp. 1799~1830.

Li, S. and Mataga, PA., 1996, "Dynamic Crack Propagation in Piezoelectric Materials - Part II. Vacuum Solution," *Journal of the Mechanics and Physics of Solids*, Vol. 44, No. 11, pp. 1831~1866.

Miller, M. K. and Guy, W. T., 1966, "Numerical Inversion of The Laplace Transform by Use of Jacobi Polynomials," *SIAM Journal on Numerical Analysis*, Vol. 3, pp. 624~635.

Narita, F. and Shindo, Y., 1998, "Scattering of Love Waves by a Surface-breaking Crack in Piezoelectric Layered Media," *JSME International Journal Series A*, Vol. 41 No. 1, pp. 40~48.

Paul, H. S. and Nelson, V. K., 1996, "Axisymmetric Vibration of Piezo-composite Hollow Circular Cylinder," *Acta Mechanica*, Vol. 116, pp. 213~222.

Shin, J. W. and Kim, T. U., 2003, "Functionally Graded Piezoelectric Strip with Eccentric Crack Under Anti-plane Shear," *KSME International Journal*, Vol. 17, No. 6, pp. 854~859.

Shin, J. W., Kim, T. U. and Kim, S. C., 2003, "Transient Response of Functionally Graded Piezoelectric Ceramic with Crack," *Journal of The Korean Society for Composite Materials*, Vol. 16, No. 5, pp. 21~27.

Shin, J. W., Kwon, S. M. and Lee, K. Y., 2001, "An Eccentric Crack in a Piezoelectric Strip Under Anti-plane Shear Impact Loading," *International Journal of Solids and Structures*, Vol. 38, pp. 1483~1494.

Shindo, Y., Katsura, H. and Yan, W., 1996, "Dynamic Stress Intensity Factor of a Cracked Dielectric Medium in a Uniform Electric Field," *Acta Mechanica*, Vol. 117, pp. 1~10.

Shindo, Y. and Ozawa, E., 1990, *Dynamic Analysis of a Piezoelectric material. In : R. K. T. Hsieh (Ed.), Mechanical modeling of new electromagnetic materials*, Elsevier Science Publishers, Amsterdam, pp. 297~304.

Xu, X.-L. and Rajapakse, R. K. N. D., 2001, "On a Plane Crack in Piezoelectric Solids," *International Journal of Solids and Structures*, Vol. 38, pp. 7643~7658.